



# Synthesis, characterization and properties of the DLC films with low Cr concentration doping by a hybrid linear ion beam system

Wei Dai, Aiyang Wang\*

Division of Surface Engineering and Remanufacturing, Ningbo Institute of Materials Technology and Engineering, Chinese Academy of Sciences, Ningbo 315201, China

## ARTICLE INFO

### Article history:

Received 1 May 2010

Accepted in revised form 26 October 2010

Available online 1 November 2010

### Keywords:

Diamond-like carbon

Low concentration doping

Residual stress

Mechanical properties

## ABSTRACT

A small amount of Cr-doped diamond-like carbon (Cr-DLC) films were deposited on silicon wafers by a hybrid deposition system composed of a DC magnetron sputtering with a Cr target (99.99% purity) and a linear ion source. Cr concentration in the films was controlled by varying the gas flow ratio of Ar/CH<sub>4</sub> in the supply gas. XPS, Raman spectroscopy, and HRTEM were employed to analyze the composition and microstructures of the films. The film residual stress was calculated via the Stoney equation, where the curvature of the film/substrate was measured by the laser reflection method. The mechanical properties and tribological behavior of the films were studied by the nano-indentor and ball-on-disc tribometer, respectively. With a small amount of Cr (<0.3 at.%) doping, the films exhibited a typical amorphous structure feature as the pure DLC film, and neither Cr–C bonding nor particulate microstructure was observed in the carbon matrix. The residual stress of the films showed a significant reduction compared with that of the pure DLC film, while the hardness of the films still retained a high value. Furthermore, the films with a low Cr content also exhibited a low friction coefficient and better wear resistance.

© 2010 Elsevier B.V. All rights reserved.

## 1. Introduction

Metal-doped diamond-like carbon (Me-DLC) films have been immensely studied recently in scientific community due to their superior toughness, thermal stability, excellent tribological properties as well as relatively lower residual stresses than that of pure DLC films [1–4]. Numerous metallic components (Ti, W, Ag, Cu, Au, etc.) have been used to modify the structures and properties of the films [5–8]. It is generally accepted that the metal atoms incorporated into the DLC matrix can form nano-clusters or bond with carbon atoms in case that the concentration of the doped metal is adequately high [9–11]. These nanostructure embedded in the DLC matrix will significantly affect the microstructure and thus the properties of the DLC films. Using a pulsed DC reactive magnetron sputtering method, Corbella et al. [12,13] investigated the effect of doped metals (including W and Mo) on the structure and properties of DLC films, and found that with a high concentration of the W and Mo doping, columnar microstructures and granular pattern structures were formed in the films. As a result, the residual stress and hardness of the films exhibited a significant decrease due to the formation of these microstructures. The particulate microstructures were also reported by Singh and co-workers [14] at a high concentration (>1.5 at.%) Cr-doped DLC films, where the formed nanoparticulates destroyed the continuity of the carbon network and led to the hardness reduction. Wang et al. [15] suggested that the

chemical state of the incorporated metal atoms significantly influenced the residual stresses of the W-DLC films synthesized by a hybrid ion beam deposition system, and the W–C bonding would increase the film residual stress at high concentration W doping.

However, it must be noted that, with a low metal doping state, those microstructures or formed carbide bonding are generally invisible, because the doped metal atoms are dispersed and dissolved in the DLC matrix displaying an amorphous microstructure [15–17]. Therefore it can be said that the doped metal atoms don't affect the microstructure by destroying the carbon network continuity but the local atomic bond distortion, and therefore the superior mechanical properties of films which depend on the carbon network will be retained. Up to now, although the studies on the low metal-doped DLC films have been reported, the comprehensive understanding of the doped metals with a lower concentration is lacking due to the complexity of carbon hybridized bonds and the diversity of doped metal nature, and the various used deposition technique as well [15]. In this work, we are focusing on the Cr-DLC films with small concentration Cr doping deposited using a unique hybrid ion beam system consisting of a DC magnetron sputtering and a linear ion source. The residual stress and mechanical properties of the films were studied, and the results indicated that the DLC films with relatively low stress and high hardness could be achieved via a low concentration Cr atoms doping.

## 2. Experimental

The low concentration Cr doping DLC films were prepared by the unique hybrid ion beam deposition system, which consists of a DC

\* Corresponding author.

E-mail address: [aywang@nimte.ac.cn](mailto:aywang@nimte.ac.cn) (A.Y. Wang).

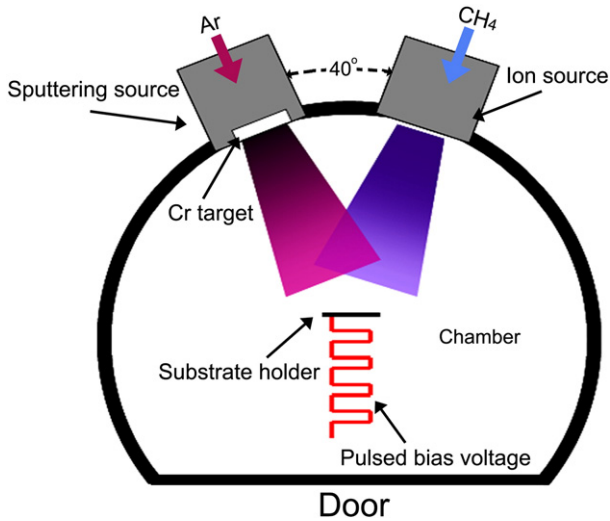


Fig. 1. Schematic diagram of the used hybrid ion beam system.

magnetron sputtering of Cr target (99.99%) and a linear ion source (LIS) supplied with  $\text{CH}_4$  for hydrogenated DLC film deposition. Fig. 1 shows the schematic diagram of the hybrid ion beam system for the present film deposition. The doped chromium concentration was controlled by varying the gas flux ratio of Ar/ $\text{CH}_4$  in the precursor gases. A p-type Si (100) wafer with thickness  $525 \pm 15 \mu\text{m}$  was used as the substrate, which was cleaned ultrasonically in acetone, ethanol, and dried in air blow before putting into the vacuum chamber. A thin Si (100) wafer of thickness  $285 \pm 5 \mu\text{m}$  was also used as a substrate to accurately estimate the residual stress. Prior to deposition, all the substrates were pre-cleaned for 10 min using Ar ions at the bias of  $-100 \text{ V}$ . The deposition chamber was evacuated to a vacuum of about  $2.66 \times 10^{-3} \text{ Pa}$  before deposition. During film deposition, the working pressure was kept at about  $4.66 \times 10^{-1} \text{ Pa}$  through a pressure control valve.  $\text{CH}_4$  gas was introduced into the linear ion source to obtain the hydrocarbon ions

and the gas flow rate was kept at 40 sccm. The voltage and current of the linear ion source were  $1050 \pm 50 \text{ V}$  and 0.2 A, respectively. Simultaneously, the Ar sputtering gas flow, ranging from 10 to 50 sccm, was supplied to the chromium magnetron sputtering. The DC power of the sputtering gun was about 1 KW ( $\sim 400 \text{ V}$ , 2.5 A). A negative pulsed bias voltage of  $-50 \text{ V}$  (350 KHz,  $1.1 \mu\text{s}$ ) was applied to the substrate during film deposition. The deposition time was adjusted to obtain a film thickness of  $550 \pm 50 \text{ nm}$  for all the samples. For comparison, the pure DLC film was prepared by only operating the linear ion source and the pure Cr film was prepared by only operating the sputter gun, respectively.

The thickness of the deposited film was measured using a surface profilometer (Alpha-Step IQ) employing a step formed by a shadow mask. The film composition was also measured by an X-ray photoelectron spectroscopy (XPS, Axis ultraDld) with Al  $\text{K}\alpha$  irradiation at a pass energy of 160 eV. Before commencing the measurement,  $\text{Ar}^+$  ion beam with an energy of 3 KeV was used to etch the sample surface for 5 min to remove contaminants. High-resolution transmission electron microscopy (HRTEM, FEI Tecnai F20) operated at 200 KeV with a point-to-point resolution of 0.24 nm was used to characterize the microstructure of the deposited film in cross-section. The TEM specimen was prepared by gluing two cut coated Si wafer slices in face-to-face, then precision and dimple grinding (Gatan Model 656), followed by Ar ion-milling at 4 KeV (Gatan Model 691). Raman spectroscopy with a 514.5 nm  $\text{Ar}^+$  laser was employed to evaluate the carbon atomic bonds of films.

The hardness and elastic modulus of the films were measured by the nano-indentation technique (MTS-G200) in a continuous stiffness measurement (CSM) mode using a Berkovich diamond tip. The maximum indentation depth was 500 nm, and the characteristic hardness was chosen in the depth of about 55 nm to minimize the substrate contribution. Six replicate indentations were made for each sample. The residual stress of the films was calculated from the curvature of the film/substrate composite using the Stoney equation, and the curvature of the film/substrate was measured by a stress tester using a laser reflection method. The tribological behavior was tested on a rotary ball-on-disc tribometer at room temperature with a

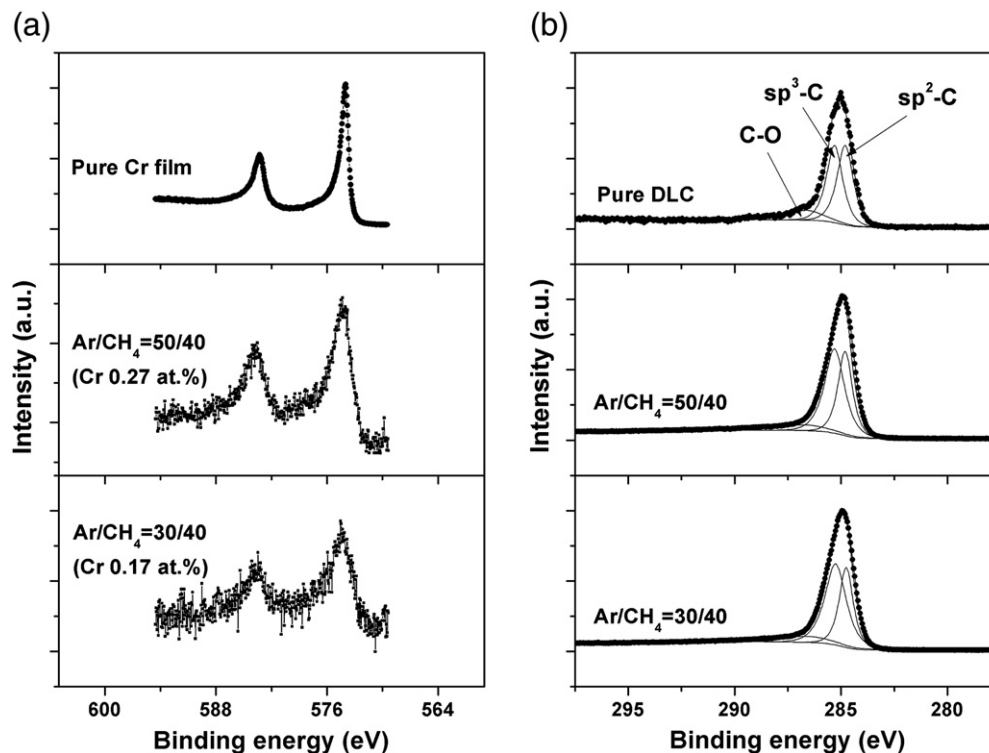


Fig. 2. Typical high-resolution XPS spectrum of the films deposited with the representative gas flux ratio of Ar/ $\text{CH}_4$ , (a) Cr 2p core level peak, and (b) C 1s core level peak of the films.

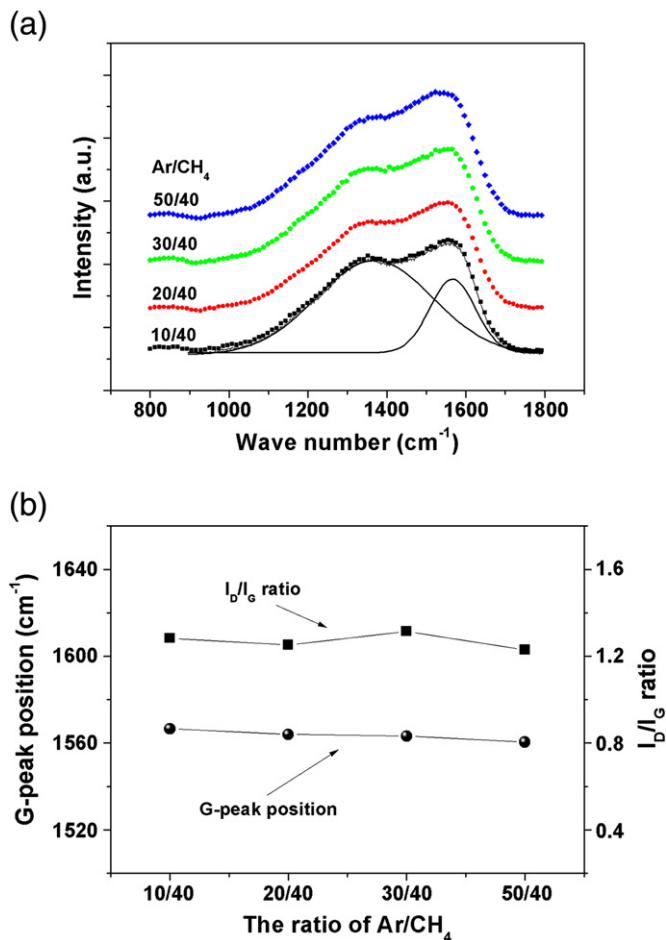


Fig. 3. (a) Typical Raman spectrum and Gaussian fitting, and (b) the corresponding G-peak position and I<sub>D</sub>/I<sub>G</sub> ratio of the films deposited with different gas flux ratios of Ar/CH<sub>4</sub>.

relative humidity of 40–50% under dry sliding conditions. A SUJ-2 steel ball (hardness-HRC60) with a diameter of 7 mm was used as the friction counter body. All the friction tests were performed under a load of 1 N with a sliding speed at 0.2 ms<sup>-1</sup>, and the total sliding distance was 500 m. After the tests, a fluorescence microscopy (Leica DM2500 M) was used to observe the wear tracks and scars.

### 3. Results and discussion

#### 3.1. Microstructural characterization

Fig. 2 shows the representative high-resolution C 1s and Cr 2p core level XPS spectra of the Cr-DLC film with the gas flow ratios of Ar/CH<sub>4</sub> at 30/40 and 50/40. For comparison, the C 1s spectrum of the pure DLC film and the Cr 2p spectrum of the pure sputtered Cr film are also included in Fig. 2(a) and (b), respectively. It can be seen from Fig. 2(a) that, all the spectra present a major peak at a binding energy around 574 eV and a shoulder peak around 583.7 eV, the intensity and the full width at half maximum of the Cr 2p peak increases with increasing the gas flow ratio of Ar/CH<sub>4</sub>. The Cr concentration, determined based on the atomic sensitivity factors and area ratio of the C 1s to Al 2p peaks in the XPS spectra of the films, increases from 0.17 to 0.27 at.% as the gas flux ratio of Ar/CH<sub>4</sub> increases from 30/40 to 50/40, and the maximum value of the doped Cr concentration is less than 0.3 at.% in the deposited films. However, it can be noted that no significant difference is observed between the Cr 2p peak in the Cr-DLC films and that in the pure sputtered Cr film. In fact, it has been reported that the Cr 2p peak cannot be used effectively to differentiate the chemical bonds between Cr and Cr carbide [14].

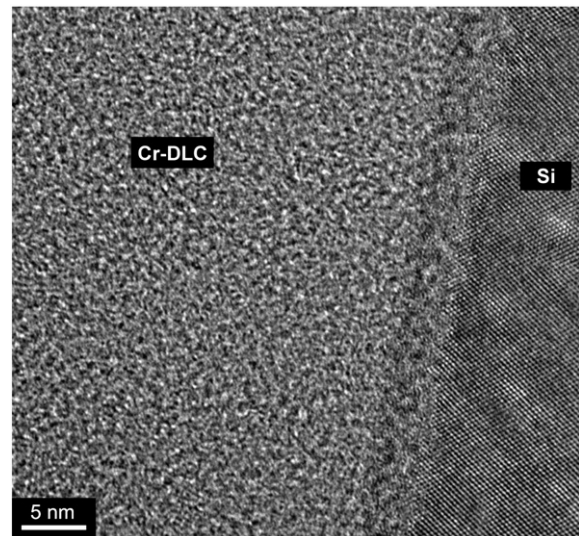


Fig. 4. Cross-sectional HRTEM of the Cr-DLC films deposited at a gas flux ratio of 50/40 (0.27 at.% of Cr).

Fig. 2(b) illustrates the corresponding high-resolution C 1s spectra of the films. There is also no distinct difference in the C 1s spectra between the pure DLC film and Cr-DLC films. In general, all the spectra present three deconvoluted peaks with binding energies at 286.1 eV for the C–O bond, 285.1 eV for sp<sup>3</sup> bonds, and 284.6 eV for sp<sup>2</sup> bonds, respectively. The reported C 1s spectra of the chromium carbides have

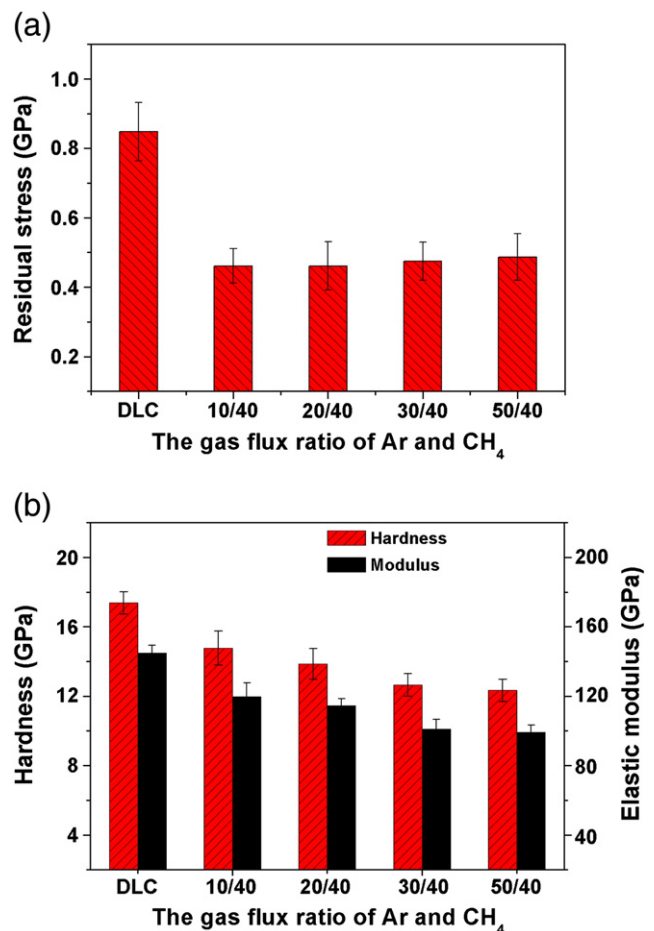


Fig. 5. (a) Residual stress, and (b) hardness and elastic modulus of the Cr-DLC films deposited at different gas flux ratio ratios.

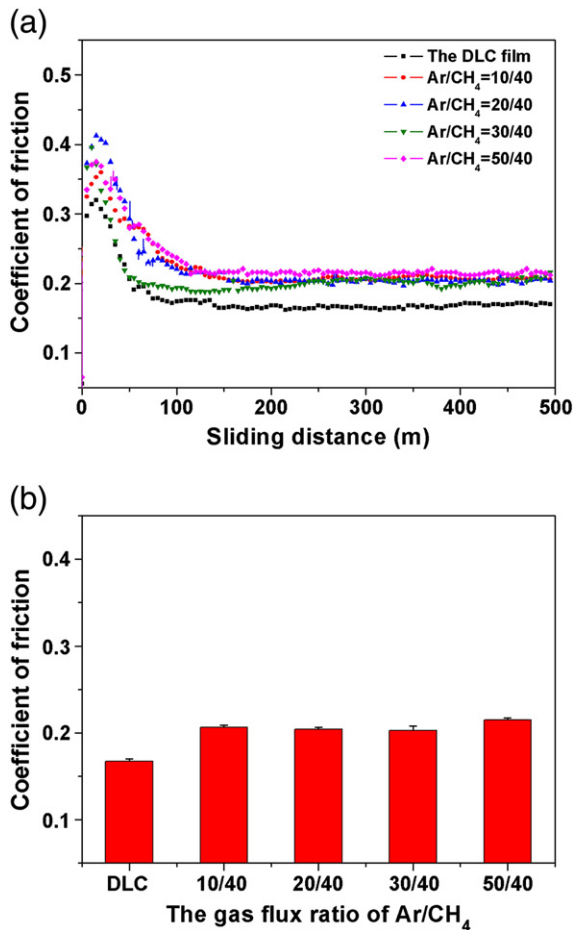


Fig. 6. (a) Friction coefficient of the films as a function of sliding distance and (b) the average friction coefficient of the films deposited with various Ar/CH<sub>4</sub> gas flux ratios.

binding energies around 283.0 eV [18,19]. Thus, the Cr atoms incorporated in the films do not bond with the carbon atoms, because of peak absence at a binding energy around 283.0 eV. Furthermore, the  $sp^3/sp^2$  ratio in the films determined by integrating the related peak area ratio in the C 1s spectra does not change a lot, demonstrating the

similar bond feature of low concentration Cr-doped DLC films as that of the pure DLC film.

Raman spectroscopy is a popular and effective tool to characterize the carbon bonding in a-C:H films. Since the  $\pi$  states have a lower energy than the  $\sigma$  states and thus are more polarisable, the  $sp^2$  sites consisting of two  $\pi$  orbits and two  $\sigma$  orbits have a 50–230 times larger Raman cross-section than  $sp^3$  sites, which only contain four  $\sigma$  orbits [20]. Accordingly, the Raman spectrum is dominated by the  $sp^2$  sites. Fig. 3(a) shows the Raman spectra of the Cr-DLC films as a function of the gas flux ratio of Ar/CH<sub>4</sub> in a wavelength range of 1000–1700  $cm^{-1}$ . All the spectra of the Cr-DLC films present an asymmetric dispersion curve, implying the typical bond feature of the amorphous hydrogenated carbon films. In visible Raman, the DLC Raman spectroscopy can be deconvoluted into two peaks: the G peak centered at around 1550  $cm^{-1}$  is due to the bond stretching of all pairs of  $sp^2$  atoms in both aromatic rings and chains, and the D peak is due to the breathing modes of  $sp^2$  atoms only in rings [20]. It is known empirically that the G-peak position will shift to higher values of wave number and  $I_D/I_G$  increases as the graphitic component in the film increases [20,21]. Fig. 3(b) shows the G-peak position and the  $I_D/I_G$  ratio of the films. The G-peak position of the films varies over a small range from 1560.4  $cm^{-1}$  to 1566.5  $cm^{-1}$  when the gas flow ratio of Ar/CH<sub>4</sub> increases from 10/40 to 50/40, while the  $I_D/I_G$  ratio almost keeps at a constant value of  $1.25 \pm 0.1$ . This indicates that the  $sp^3/sp^2$  ratio of the films has little change as the Ar/CH<sub>4</sub> ratio increases.

Fig. 4(a) presents the cross-sectional HRTEM micrograph of the Cr-DLC film (Cr 0.27 at.%) deposited with the gas flow ratio of Ar/CH<sub>4</sub> at 50/40. It is seen that nano-crystalline and particulate, as shown in previous papers [14,15], are not found in the film. The corresponding selected area diffraction (SAED) pattern of the film also exhibits a diffuse halo without any observable diffraction rings. Those results illustrate that at low doping levels (<0.3 at.%), Cr atoms are uniformly distributed and dissolve in the DLC matrix, and the as-deposited Cr-DLC films perform a typical amorphous structure.

### 3.2. Stress and mechanical characterization

Fig. 5(a) shows the residual stresses of the films. All the Cr-DLC films exhibit a lower residual stress compared with the pure DLC film deposited by the linear ion source, and the residual stress stabilizes around 0.46 GPa as the gas flux ratio of Ar/CH<sub>4</sub> increases further. Two main aspects should be taken into account for the reduction of the residual stress. On one hand, the Cr<sup>+</sup> bombardment of the magnetron

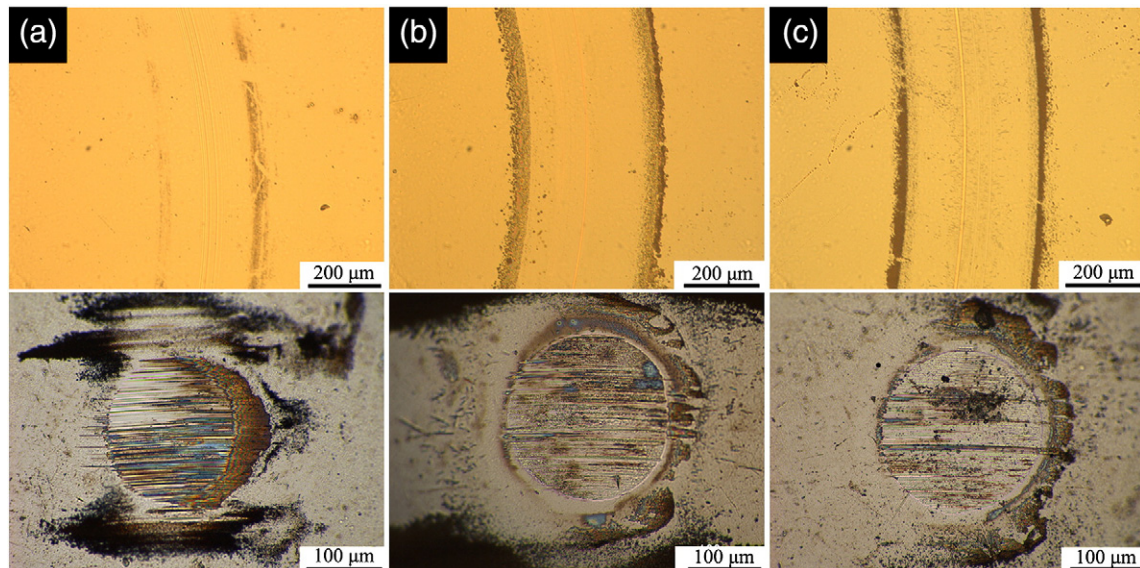


Fig. 7. Wear surfaces (upper) of the films deposited with the gas flux ratio of Ar/CH<sub>4</sub> at (a) 0/40, (b) 10/40 and (c) 30/40, and the corresponding contact balls after the friction test (lower).

sputtering source will increase the adatom mobility, which has been expected to contribute to the relaxation of the residual stress of the film [22,23]. On the other hand, it was found that at a low doping level, the metal atoms distributed in the DLC matrix without bonding with carbon can result in the atomic bond distortion, which will decrease the residual stress of the film [15,24].

Fig. 5(b) shows the hardness and elastic modulus of the films. The hardness and elastic modulus decrease continuously with increasing the Ar/CH<sub>4</sub> gas flux ratio, but the decrease degree is very small. Normally, the mechanical properties of DLC films mainly depend on the sp<sup>3</sup> carbon matrix [20]. According to the XPS and Raman spectrum results, although a small amount of Cr atoms are incorporated, the atomic bond structure of carbon (the bonding ratio of sp<sup>3</sup>/sp<sup>2</sup>) keeps constant without any obvious change. Therefore, the reduction of the film hardness may be attributed to the increase of the plasticity due to the Cr doping. It was found that the incorporation of the metal atoms would cause the plasticity of DLC films to increase [3,25]. Note that the hardness of the films still retains a high value (>12 GPa), although the residual stress of the films decreases to a low value of about 0.46 GPa. This indicates that the DLC films with relatively low stress and high hardness can be acquired through low concentration metal atoms doping using the hybrid beams.

### 3.3. Tribological behavior

Fig. 6(a) reveals the evolution of the friction coefficient of the DLC film and Cr-DLC films against the sliding distance, and the average friction coefficients (calculated after 200 m of sliding distance) of the deposited films are also given in Fig. 6(b). It shows that, in general, the Cr-DLC films exhibit a low coefficient of friction against SUJ-2 steel ball and slightly higher than the pure DLC film. As the gas flux ratio of Ar/CH<sub>4</sub> increases, the friction coefficient of the Cr-DLC films has no significant change. Fig. 7 shows the wear surfaces on the films and the corresponding contact balls after the friction test. Obviously, the wear track and wear scar of the Cr-DLC films are slightly larger than those of the DLC film, implying that the Cr-DLC films perform more serious wear compared with the pure DLC film. The wear rate of the Cr-DLC films is about  $3 \times 10^{-8}$  mm<sup>3</sup>/Nm, which is higher than that of the pure DLC film of about  $2.6 \times 10^{-8}$  mm<sup>3</sup>/Nm. The film tribological behavior may have a relationship with the hardness, which decreases with the incorporation of Cr atoms, as shown above. Even so, the Cr-DLC films still possess a low friction coefficient and will be a good candidate for the tribological application.

## 4. Conclusions

Diamond-like carbon films with low concentration Cr doping (<0.3 at.%) were deposited by a hybrid beam system, which is composed of a DC magnetron sputtering and a linear ion source. The Cr concentration in the deposited films was adjusted by varying the gas flux ratio of Ar and CH<sub>4</sub> in the supply gas. In the present

concentration (<0.3 at.%), neither Cr-C bonding nor particulate microstructure are observed in the as-deposited films, and the film carbon structure (sp<sup>3</sup>/sp<sup>2</sup> ratio) almost keeps constant without any obvious change. The residual stresses of the films show a significant decrease compared with that of the pure DLC film due to the atomic bond distortion and the enhancement of the adatom mobility induced by Cr ion bombardment. The hardness of the films decrease slowly with increasing Ar/CH<sub>4</sub> gas flux ratio, but it still retains a high hardness (<12 GPa), which is mainly caused by the relatively stable carbon structure (sp<sup>3</sup>/sp<sup>2</sup> ratio). The films with low concentration Cr doping also exhibit excellent tribological properties with a wear rate of about  $3 \times 10^{-8}$  mm<sup>3</sup>/Nm and a friction coefficient of about 0.2, which are slightly higher than that of the pure DLC film.

## Acknowledgements

The project was supported by the Zhejiang Province Key Technologies R & D Program (Grant No. 2008C21055 and 2009C11SA550048), the Foundation of State Key Laboratory of Solid Lubrication, Lanzhou Institute of Physics and Chemistry, Chinese Academy of Science, and the Natural Science Foundation of China (Grant No: 51072205).

## References

- [1] X.Z. Ding, B.K. Tay, S.P. Lau, P. Zhang, X.T. Zeng, *Thin Solid Films* 408 (2002) 183.
- [2] Y. Pauleau, F. Thiéry, *Surf. Coat. Technol.* 180 (2004) 313.
- [3] K.I. Schiffmann, *Surf. Coat. Technol.* 177–178 (2004) 453.
- [4] K. Bewilogua, R. Wittorf, H. Thomsen, M. Weber, *Thin Solid Films* 447–448 (2004) 142.
- [5] Y.T. Pei, C.Q. Chen, K.P. Shaha, M.J.Th. De Hosson, J.W. Bradley, S.A. Voronin, M. Cada, *Acta Mater.* 56 (2008) 696.
- [6] A. Czyzniewski, *Thin Solid Films* 433 (2003) 180.
- [7] H.W. Choi, J.H. Choi, K.R. Lee, J.P. Ahn, K.H. Oh, *Thin Solid Films* 516 (2007) 248.
- [8] I. Gerhards, C. Ronning, U. Vetter, H. Hofsäss, H. Gibhardt, G. Eckold, Q. Li, S.T. Lee, Y.L. Huang, M. Seibt, *Surf. Coat. Technol.* 158 (2002) 114.
- [9] V. Singh, V. Palshin, R.C. Tittsworth, E.I. Meletis, *Carbon* 44 (2006) 1280.
- [10] C. Strondl, N.M. Carvalho, J.Th.M. De Hosson, G.J. van der Kolk, *Surf. Coat. Technol.* 162 (2003) 288.
- [11] B. Feng, D.M. Cao, W.J. Meng, J. Xu, R.C. Tittsworth, L.E. Rehn, P.M. Baldo, G.L. Doll, *Surf. Coat. Technol.* 148 (2001) 153.
- [12] C. Corbella, E. Bertran, M.C. Polo, E. Pascual, J.L. Aandújar, *Diamond Relat. Mater.* 16 (2007) 1828.
- [13] C. Corbella, G. Oncins, M.A. Gómez, M.C. Polo, E. Pascual, J. Garcia-Céspedes, J.L. Aandújar, E. Bertran, *Diamond Relat. Mater.* 14 (2005) 1103.
- [14] V. Singh, J.C. Jiang, E.I. Meletis, *Thin Solid Films* 489 (2005) 150.
- [15] A.Y. Wang, K.R. Lee, J.P. Ahn, J.H. Han, *Carbon* 44 (2006) 1826.
- [16] X. Han, F. Yan, A. Zhang, P. Yan, B. Wang, W. Liu, Z. Mu, *Mater. Sci. Eng. A348* (2003) 319.
- [17] S. Zhang, X.L. Bui, J. Jiang, X. Li, *Surf. Coat. Technol.* 198 (2005) 206.
- [18] H. Goretzki, Z. Fres, *Anal. Chem.* 333 (1989) 451.
- [19] L. Ramqvist, *J. Phys. Chem. Solids* 30 (1969) 1835.
- [20] J. Robertson, *Mater. Sci. Eng. R* 37 (2002) 129.
- [21] C. Casiraghi, A.C. Ferrari, J. Robertson, *Phys. Rev. B* 72 (2005) 085401.
- [22] X.L. Peng, T.W. Clvne, *Thin Solid Films* 312 (1998) 207.
- [23] Y.N. Kok, P.Eh. Hovsepian, Q. Luo, D.B. Lewis, J.G. Wen, I. Petrov, *Thin Solid Films* 475 (2005) 219.
- [24] A.Y. Wang, H.S. Ahn, K.R. Lee, J.P. Ahn, *Appl. Phys. Lett.* 86 (2005) 111902.
- [25] S.J. Harris, A.M. Weiner, W.J. Meng, *Wear* 211 (1997) 208.